fective the lower the concentration of the permeant on the dark side of the membrane.

The concentration difference produced by a photodiffusion membrane system represents potential energy that can be stored in a coupled system or utilized in the form of work; by this mechanism photodiffusion membranes can provide an approach to the capture and utilization of solar energy.

Indirect photodiffusion membranes. Similar effects can be produced with permeants whose binding reactions with the carrier species are not photochromic, provided competing species can be found whose reaction with the carrier is photochemically activated. This is one form of photosensitization. For example, consider the system O_2, CO, and myoglobin. It is known that the quantum efficiency of light for dissociation of carboxyhemoglobin is about 0.4 (*10*), whereas that for dissociation of oxymyoglobin is 100 times lower. However, because both O_2 and CO compete for the same carrier, the light sensitivity of the CO reaction can be used to effect the concentration of O_2 across a photodiffusion membrane. The equation for O_2 transport across a myoglobin (Mb) membrane in the presence of CO under reaction equilibrium conditions is

$$N_{O_2} = \frac{D_{O_2}}{d}([O_2]_I - [O_2]_{II}) + \frac{D_{Mb}}{d}[Mb]_t K\left(\frac{[O_2]_I}{1 + K[O_2]_I + L_I[CO]_I} - \frac{[O_2]_{II}}{1 + K[O_2]_{II} + L_{II}[CO]_{II}}\right) \quad (5)$$

In this case the binding constant, K, for O_2 to myoglobin is the same on both sides of the film, whereas the association constant for CO-myoglobin can be altered by differential illumination. Inspection of Eq. 5 shows that under conditions where $L_I \neq L_{II}$, an O_2 flux across the membrane can be induced even if the ambient concentrations of this nonphotochemically sensitive species are equal on both sides of the membrane. For example, if equal O_2 and CO partial pressures were maintained on both sides of the membrane, the expected concentration profiles that would develop within the membrane are as illustrated in Fig. 2c, and the net flux of O_2 across the membrane would be from the illuminated to the dark side.

We have demonstrated this indirect coupling of O_2 transport to illumination in some preliminary experiments, using hemoglobin as the carrier species. A membrane sandwich (as described in Fig. 2) was placed in contact with an O_2-sensing electrode in a CO-O_2-N_2 gas environment. When one side of the membrane was illuminated, the O_2 electrode indicated an increase in the O_2 concentration on the dark side of the membrane. The effect was reversible.

JEROME S. SCHULTZ
Department of Chemical Engineering, University of Michigan, Ann Arbor 48109

References and Notes

1. P. F. Scholander, *Science* **131**, 585 (1960); G. M. Shean and K. Sollner, *Ann. N.Y. Acad. Sci.* **137**, 759 (1966); W. J. Ward and W. L. Robb, *Science* **156**, 1481 (1967); C. Pressman, *Fed. Proc. Fed. Am. Soc. Exp. Biol.* **27**, 1283 (1968).
2. J. S. Schultz, J. D. Goddard, S. R. Suchdeo, *AIChE J.* **20**, 417 (1974); J. D. Goddard, J. S. Schultz, S. R. Suchdeo, *ibid.*, p. 625.
3. D. R. Olander, *ibid.* **6**, 233 (1960); J. D. Goddard, J. S. Schultz, R. J. Bassett, *Chem. Eng. Sci.* **20**, 121 (1965).
4. S. K. Freidlander and K. H. Keller, *Chem. Eng. Sci.* **20**, 121 (1965); R. Blumenthal and A. Katchalsky, *Biochim. Biophys. Acta* **173**, 357 (1969); F. Kreuzer and L. J. C. Hoofd, *Respir. Physiol.* **8**, 380 (1970); K. A. Smith, J. K. Meldon, C. K. Colton, *AIChE J.* **19**, 102 (1973).
5. J. Haldane and J. Lorrain-Smith, *J. Physiol. (London)* **20**, 497 (1895).
6. C. Bonaventura *et al.*, *Biochemistry* **12**, 3424 (1973).
7. M. Mochizuki and R. E. Forster, *Science* **138**, 897 (1962).
8. The experimental evidence shown in Fig. 2 confirms the observations of Mochizuki and Forster (*7*) on the facilitated transport of CO by hemoproteins. J. B. Wittenberg [*J. Biol. Chem.* **241**, 104 (1966)] was unable to demonstrate this effect, and others proposed mathematical analyses to try to prove that CO facilitation could not be obtained in practice [J. D. Murray and J. Wyman, *J. Biol. Chem.* **246**, 5903 (1971); P. Mitchell and J. D. Murray, *Biophysik* **9**, 177 (1973)].
9. The equations in this report are based on simple unimolecular binding behavior. In other cases, the actual equilibrium binding functions should be used. For example, in the CO-hemoglobin system of Fig. 2, the saturation function, Y_{CO} can be represented by the Hill equation (*10*)

$$Y_{CO} = \frac{{p_{CO}}^n}{{p_{50}}^n + {p_{CO}}^n}$$

where p_{CO} is the partial pressure of CO, p_{50} is the partial pressure of CO that gives half saturation, n is the Hill constant, and both n and p_{50} may be functions of light intensity. In this case Eq. 1 becomes

$$N_{CO} = \frac{D_{CO}H_{CO}}{d}(p_{CO_I} - p_{CO_{II}}) + \frac{D_{Hb}4[Hb]_t}{d}(Y_{CO}{}^{I} - Y_{CO}{}^{II})$$

where H_{CO} is the solubility of CO in water.
10. E. Antonini and M. Brunori, *Hemoglobin and Myoglobin in Their Reactions with Ligands* (North-Holland, Amsterdam, 1971).
11. Supported in part by NIH grant GM-15152, Research Career Development Award 1KOGM08271, and the Volkswagen Werke Foundation. The assistance of K. Murai, R. Deno, and M. Flessner in obtaining the data of Fig. 2 is gratefully acknowledged.

15 March 1977; revised 31 May 1977

Long Waves in the Eastern Equatorial Pacific Ocean: A View from a Geostationary Satellite

Abstract. *During 1975, westward-moving long waves with a period of about 25 days and a wavelength of 1000 kilometers were observed at a sea surface temperature front in the equatorial Pacific on infrared images obtained by a geostationary environmental satellite system. The absence of these waves during 1976, and the above-average equatorial sea surface temperatures during 1976, may be related to a decrease in the southeasterly trade winds during that year.*

The major components of the current system in the tropical oceans are the alternating bands of eastward- and westward-flowing currents in the surface layers. Although the existence of these currents has been known for a considerable time, very little information is available about their variability. For example, one of the principal results of the multiship experiment conducted in the tropical Atlantic during the summer of 1974 was the discovery that the Atlantic equatorial currents have fluctuations with a period of about 16 days. The phase speed of these oscillations is in a westward direction, and a wavelength of 2500 km has been estimated by Düing *et al.* (*1*). Recent measurements by Harvey and Patzert (*2*) near the ocean floor in the eastern tropical Pacific show current fluctuations that suggest westward-propagating waves with a wavelength of about 1000 km and a period of approximately 25 days. I present here evidence, obtained by a geostationary environmental satellite (*3*), that there are similar westward-propagating long waves in the surface layers of the eastern equatorial Pacific.

The westward flow in the vicinity of the equator is part of the South Equatorial Current. It is associated with low temperatures because of equatorial upwelling and the advection of cold water from the coast of South America. The neighboring current to the north, the eastward North Equatorial Countercurrent, advects relatively warm water from the west. The boundary between these currents is associated with large latitudinal temperature gradients, especially in the eastern Pacific. The gradients are sufficiently large for the associated thermal front (*4*) to be visible on infrared satellite images such as those shown in Fig. 1, a through d. The relatively colder water (lighter shades of

gray) is centered along the equator, and a sharp transition to warmer water (2° to 4°C in about 50 km) occurs between 1°N and 3°N. The most striking feature in these images is the wavelike structure of the temperature front which has sharp peaks (labeled B, C, and D in Fig. 1) and long troughs. These wave peaks move westward with time.

Although the long waves were first detected by satellite in May 1975, it was not possible to obtain an adequate time series of the waves until October and November. During these 2 months the north-south temperature gradients along the equatorial front were most intense and the available satellite images were sufficiently distinct, and so it was possible to resolve the wave motions with time. Figure 1f shows the distance between pairs of wave peaks as a function of time. This distance, which is effectively a wavelength, decreases from about 1200 to 800 km while the phase speed averages about 40 km/day. From this one can infer that the period of the phenomenon at a given point is of the order of 20 to 30 days.

Whereas the oceanic temperature front was observed most clearly in October and November 1975, the southeasterly trade winds over the eastern tropical Pacific were most intense 1 to 2 months earlier, in September. This is evident from Fig. 2, which shows the mean monthly wind speed, averaged over the latitude band from the equator to 25°S along 100°W, as derived from satellite-observed cloud motions at a height of 1000 m (*5*). Ship measurements (*6*) confirm that there is a lag of 1 to 2 months between the time of the most intense trade winds in 1975 and the time of the lowest equatorial water temperatures between 100°W and 140°W. This continued decrease of the temperature, after the winds have diminished, cannot be attributed to equatorial upwelling alone and suggests that colder water is being advected from the east by the South Equatorial Current. Ship measurements

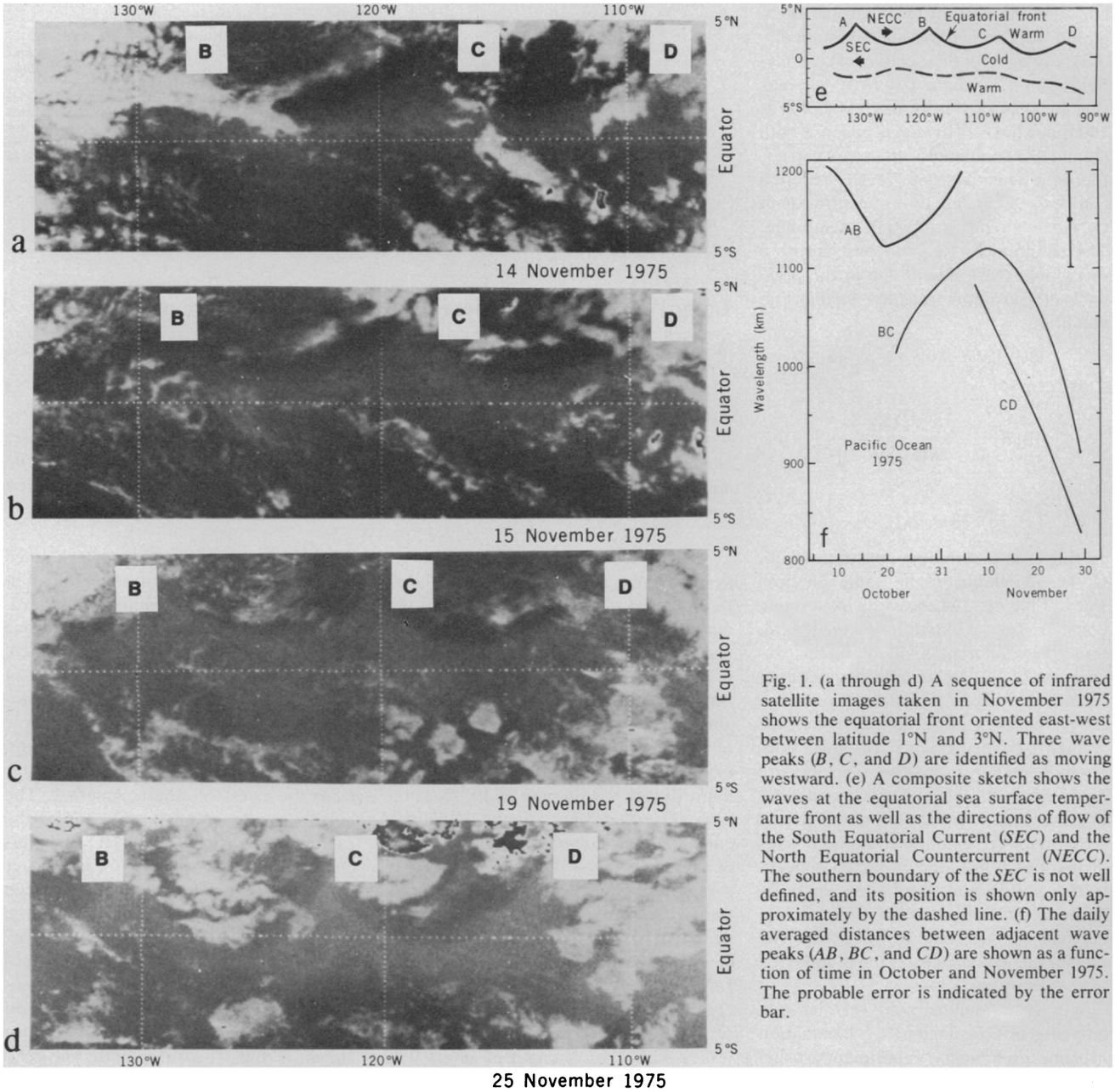

Fig. 1. (a through d) A sequence of infrared satellite images taken in November 1975 shows the equatorial front oriented east-west between latitude 1°N and 3°N. Three wave peaks (*B*, *C*, and *D*) are identified as moving westward. (e) A composite sketch shows the waves at the equatorial sea surface temperature front as well as the directions of flow of the South Equatorial Current (*SEC*) and the North Equatorial Countercurrent (*NECC*). The southern boundary of the *SEC* is not well defined, and its position is shown only approximately by the dashed line. (f) The daily averaged distances between adjacent wave peaks (*AB*, *BC*, and *CD*) are shown as a function of time in October and November 1975. The probable error is indicated by the error bar.

(6) also confirm that sea surface temperatures in the eastern equatorial Pacific decreased in a westward direction between March and November 1975.

After measurement of the equatorial wave motions during 1975, it was expected that similar satellite observations could be made each year. During 1976, however, neither the equatorial front nor the long waves were detectable in the satellite imagery. The reason is probably related to the anomalous winds and sea surface temperatures reported in the eastern equatorial Pacific during 1976. From Fig. 2 it is evident that the southeasterly trade winds were considerably weaker in 1976 than in 1975. Ship measurements (6) show that the eastern equatorial Pacific sea surface temperatures between 5°N and 5°S were higher by 4° to 6°C in 1976 than in 1975. Similar anomalously warm water was observed in 1972, 1965, and 1957 in connection with the so-called El Niño. According to Wyrtki (7), excessively strong southeasterly trade winds, during the year preceding the El Niño, increase the east-west slope of sea level by building up water in the western equatorial Pacific. When the winds relax, as during 1976 (see Fig. 2), the accumulated water flows eastward and leads to equatorial warming that extends to the coast of Peru.

Although the limitations of the available satellite images prevented the detection of the motion of the equatorial front during 1976, there is reason to believe that equatorial waves were indeed present. Hansen (8) reports that surface drifter buoys in the North Equatorial Countercurrent (latitude 6°N) followed a meandering eastward path from 150°W to 130°W from December 1975 to March 1976. These observations suggest that the waves observed by satellite during 1975 persisted for at least 3 months in 1976. Although similar time and space scales appear in the data acquired by these different observational methods, simultaneous measurements must be made to properly compare the data. Efforts are presently under way to improve the enhancement of satellite images so that the equatorial front can be detected even when the sea surface temperature gradients are relatively weaker.

One plausible explanation for the westward motion of the waves appears to be that advanced by Philander (9). On the basis of a linear stability analysis of equatorial currents, he predicted that the large latitudinal shear between the South Equatorial Current and the North Equatorial Countercurrent in the Pacific will result in unstable waves with temporal and spatial scales close to the values observed by satellite. Philander (10) has also suggested that the waves observed near the ocean floor by Harvey and Patzert (2) could be neutral waves (equatorially trapped Rossby-gravity waves, for example) that are excited by the instability in the surface layers of the ocean and that propagate vertically downward to the ocean floor. This would explain why the waves observed there and those observed by satellite have the same period and wavelength.

If the long waves in the equatorial Pacific are indeed due to an instability of the currents, then it should be possible to relate their period and wavelength to the shear and hence intensity of the currents. It may be possible to monitor the equatorial currents by measuring the period and wavelength of the waves by satellite. To explore this relation, simultaneous measurements by satellite and by in situ ocean instruments are required.

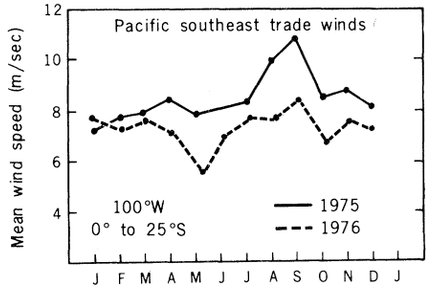

Fig. 2. The southeasterly wind speed during 1975 and 1976 is shown at longitude 100°W as a monthly mean between latitudes 0° and 25°S. These speeds were measured from satellite-observed cloud motions at 900 mbar (approximately 1000 m).

RICHARD LEGECKIS

National Environmental Satellite Service, National Oceanic and Atmospheric Administration, Washington, D.C. 20233

References and Notes

1. W. Düing *et al.*, *Nature (London)* **257**, 280 (1975).
2. R. R. Harvey and W. Patzert, *Science* **193**, 883 (1976).
3. The geostationary operational environmental satellite (GOES) rotates with the earth at a speed which maintains the satellite stationary over the same area of the earth. Observations are made at 30-minute intervals at the visible (0.5 to 0.75 μm) and thermal infrared (10.5 to 12.5 μm) wavelengths. The GOES is operated by the National Environmental Satellite Service (NESS).
4. I thank F. C. Parmenter of the Applications Group (NESS) for calling to my attention the equatorial ocean front.
5. M. T. Young, *Natl. Oceanic Atmos. Adm. Tech. Memo NESS 64* (1975).
6. *Fishing Information* (National Marine Fisheries Service, National Oceanic and Atmospheric Administration, La Jolla, Calif.).
7. K. Wyrtki, *J. Phys. Oceanogr.* **4**, 372 (1974).
8. D. Hansen, personal communication.
9. S. G. H. Philander, *J. Geophys. Res.* **81**, 3725 (1976). The stability analysis described in this paper is for equatorial currents that only crudely resemble the observed currents. The analysis predicts unstable waves with a period of 2 to 3 weeks and a wavelength of about 2000 km. More recent calculations (*10*) show that the characteristic scales are sensitive to the latitudinal profile of the mean flow. In particular, a narrow shear zone between the South Equatorial Current and the North Equatorial Countercurrent leads to shorter waves and longer periods.
10. ———, in preparation.

11. I thank S. G. H. Philander for his many suggestions and encouragement in the preparation of this report.

22 October 1976; revised 29 March 1977

Timekeeping by the Pineal Gland

Abstract. *N-Acetyltransferase, an enzyme involved in melatonin production in the pineal gland, exhibits a circadian rhythm in chickens with peak values in the dark-time and low values during the light-time, commencing at lights-on. When pineal glands of chickens killed during the dark-time (with high N-acetyltransferase activity) were organ-cultured, there was a decline in enzyme activity to light-time values. Regardless of the time of the dark at which the chickens were killed, the enzyme activity reached light-time levels at precisely the same time.*

Investigators studying house sparrows have demonstrated a physiological role for the pineal gland in circadian rhythms. Pinealectomy, pineal transplants to the anterior chamber of the eye, and melatonin implants provide a convincing case that supports the idea that the pineal gland may be the source of the circadian locomotor rhythm in house sparrows. Furthermore, melatonin, a pineal hormone, may be the means by which rhythmic signals are transmitted to the brain or body of the sparrow (or both) (*1*). Not only is there evidence that the pineal gland may function as a biological clock, but also there is good evidence that the pineal gland has rhythms in melatonin and in the activity of the enzyme involved in melatonin synthesis, *N*-acetyltransferase. *N*-acetyltransferase activity exhibits a daily rhythm in house sparrows and other vertebrates. We have studied in detail the rhythms in *N*-acetyltransferase activity in vivo in chickens, and we have paid special attention to regulation by light and dark: the daily cycle (27-fold in a light-dark cycle) persists in constant dark; the rhythm is damped by constant light; the shape of the oscillation is modified by